Ocean Sci. Discuss., 7, 1913–1951, 2010
www.ocean-sci-discuss.net/7/1913/2010/
doi:10.5194/osd-7-1913-2010

Ocean Science Discussions

Upper ocean stratification and sea ice growth rates during the summer-fall transition, as revealed by Elephant seal foraging in the Adélie Depression, East Antarctica

G. D. Williams[1,2], M. Hindell[3], M.-N. Houssais[1], T. Tamura[2], and I. C. Field[4]

[1]LOCEAN, UMR7159 CNRS/UPMC/IRD/MNHN, Université Pierre et Marie Curie, 4 place Jussieu, Paris, France
[2]ACE CRC, University of Tasmania, Private Bag 80 Hobart TAS 7001, Australia
[3]IMAS, University of Tasmania, Private Bag 129, Hobart TAS 7001, Australia
[4]Graduate School of the Environment, Macquarie University, North Ryde NSW, 2109 Australia

Received: 15 October 2010 – Accepted: 22 October 2010 – Published: 16 November 2010

Correspondence to: G. D. Williams (guy.darvall.williams@gmail.com)

Published by Copernicus Publications on behalf of the European Geosciences Union.

Abstract

Southern elephant seals (*Mirounga leonina*), fitted with Conductivity-Temperature-Depth sensors at Macquarie Island in January 2005 and 2010, collected unique oceanographic observations of the Adélie and George V Land continental shelf (140–148° E) during the summer-fall transition (late February through April). This is a key region of dense shelf water formation from enhanced sea ice growth/brine-rejection in the local coastal polynyas. In 2005 two seals occupied the continental shelf break near the grounded icebergs at the northern end of the Mertz Glacier Tongue for nearly two weeks at the onset of sea ice growth. One of the seals migrated north thereafter and the other headed west, possibly utilising the Antarctic Slope Front current near the continental shelf break. In 2010, after that years calving of the Mertz Glacier Tongue, two seals migrated to the same region but penetrated much further southwest across the Adélie Depression and occupied the Commonwealth Bay polynya from March through April. Here we present unique observations of the regional oceanography during the summer-fall transition, in particular (a) the zonal distribution of modified Circumpolar Deep Water exchange across the shelf break, (b) the upper ocean stratification across the Adélie Depression, including alongside iceberg C–28 that calved from the Mertz Glacier and (c) the convective overturning of the deep remnant seasonal mixed layer in Commonwealth Bay from sea ice growth (7.5–12.5 cm s^{-1}). Heat and freshwater budgets to 200–300 m are used to estimate the ocean heat content, heat flux and sea ice growth rates. We speculate that the continuous foraging by the seals within Commonwealth Bay during the summer-fall transition was due to favorable feeding conditions resulting from the convective overturning of the deep seasonal mixed layer and chlorophyll maximum that is a reported feature of this location.

OSD

7, 1913–1951, 2010

1 Introduction

One of the key challenges facing the global ocean climate modelling community, in particular in the Southern Ocean around Antarctica, is the scarcity of oceanographic observations that adequately describe the temporal and spatial variability. The introduction of the ARGOS float program has made great steps to address this imbalance, supplying near real-time data on the ocean state. In association with this technology has come the deployment of similar instruments on marine mammals, birds and fish, which have proven very successful in collecting complementary and unique datasets to the ARGO float program (see Biuw et al. (2007); Boehme et al. (2008); Charrassin et al. (2008); Costa et al. (2008); Meredith et al. (2010) and references therein). The standard ARGO floats do not extend into the sea ice zone and whilst the newly developed and recently deployed Ice-ARGO floats can, these are still limited to the north of the continental slope (ocean depths greater than 2000 m). The most sparsely-observed and logistically difficult region is the coastal region south of the continental shelf break. In this region, at specific seasons, biologically-mounted observation platforms are often the only source of in situ data.

Female elephant seals (*Mirounga leonina*) equipped with oceanographic sensors provide valuable observations on the environment, and the biological responses to its variability, around the Southern Ocean (Biuw et al., 2007; Bailleul et al., 2007). In the Australian/South Indian sector, southern elephant seals from Macquarie Island were tagged as part of the Southern Elephant as Oceanographic Samplers (SEaOS, http://biology.st-andrews.ac.uk/seaos/) and Integrated Marine Observing Systems through the Australian Animal Tracking and Monitoring System facility (IMOS/AATMS, hereafter IMOS – http://imos.org.au/aatams.html) programs. Nine and fifteen animals were tagged in 2005 (SEaOS) and 2010 (IMOS), respectively. Their annual migration south covered a wide region (see Fig. 1). The most unique data from the SEaOS and IMOS seals was collected on the continental shelf after the beginning of the sea ice growth season. Of particular interest is the data collected from the Adélie and George V land

OSD
7, 1913–1951, 2010

(hereafter collectively referred to as AGV) region of East Antarctica (140–148° E, see Fig. 2), which is a key formation region for the dense shelf water precursor to the Antarctic Bottom Water (AABW) produced in this sector (Gordon and Tchernia, 1972; Rintoul, 1998; Whitworth III, 2002).

Dense shelf water is formed during the austral winter (April–October) via brine rejection from enhanced sea ice formation in the coastal polynyas of this region (Williams et al., 2008a). When suffiently dense and successfully exported north across the shelf break, this water mass mixes down the AGV continental slope to produce a local variety of Antarctic Bottom Water to the Australian-Antarctic Basin (Williams et al., 2010a). Recent observational programs using standard ship-based CTD surveys and moored instrument arrays have described the seasonal cycle of water mass transformation in the Adélie Depression (Williams and Bindoff, 2003; Williams et al., 2008a). These observations have been essential for validating models seeking to predict the future sensitivity of dense shelf export from this region (Marsland et al., 2004, 2007; Kusahara et al., 2010a,b) and studies seeking to groundtruth estimates of sea ice production from satellite data (Tamura et al., 2008). Nonetheless logistic constraints have led to spatial and temporal gaps in the observations and consequently our understanding of the oceanography.

In this paper we detail new, unique oceanographic measurements for the Adélie Depression during the summer/fall transition from the SEaOS (Feb.–Mar. 2005) and IMOS (Feb.–Apr. 2010) deployments. In Sect. 2 we provide the background to the study region and its oceanography. Sect. 3 details the data and methods. Section 4 presents the seal-mounted CTD data and describes: the seasonal variability in the zonal distribution of modified Circumpolar Deep Water intrusions; the vertical stratification across the Adélie Depression at the end of summer; and the re-conditioning of the remnant summer mixed layer at the start of the sea ice growth season in Commonwealth Bay from late February through April. We use the repeat profiling by the IMOS seals in Commonwealth Bay to estimates ocean heat content, heat flux and daily sea ice growth rates from heat and freshwater budgets in the upper 200–300 m. In Sect. 5

OSD
7, 1913–1951, 2010

we compare the sea ice growth rates to satellite derived analyses and discuss new insights gained into the oceanographic processes of the region and speculate on how the seals are utilising these to benefit their foraging strategy.

2 The Adélie and George V land continental shelf

2.1 Bathymetry and Glacial features

Our study area is the Adélie Depression and surrounds (see Fig. 2), situated across the transition from Adélie Land (136–142° E) to George V Land (142–153° E). The Adélie Depression (AD), also referred to as the Mertz–Ninnis Trough, was formed during a previous extension of the continental ice sheet. The major cryospheric features are the floating extension of the Mertz Glacier Tongue (MGT), which prior to its calving in February 2010 extended nearly 100 km across the AD and onto the continental shelf break, and the enhanced sea ice produced in the coastal polynyas that form each winter. Historically the sea ice formation over the Adélie Depression has been collectively referred to as the Mertz Glacier Polynya. More recently there has been a sub-regionalisation distinguishing between the polynya in the western lee of the MGT and grounded icebergs to the north and the polynyas in the coastal bays to the west, namely Buchanan Bay, Watt Bay and Commonwealth Bay (from east to west). Massom et al. (2001) suggested that along the coast the polynyas were more influenced by the katabatic wind system draining from the continent and that the polynya in the lee of the MGT was more influenced by synoptic systems.

Commonwealth Bay, infamously known as 'Home of the Blizzard' (Mawson, 1930), is globally the windiest sea-level location, with mean annual wind speeds of $\sim$20 ms^{-1} (Parish and Wendler, 1991; Adolphs and Wendler, 1995). Bathymetrically Commonwealth Bay is partially isolated from the greater Adélie Depression. Divided zonally, the main region of open water associated with the polynya is over relatively shallow coastal bathymetry in the east. The western sector has a more complex bathymetry,

OSD
7, 1913–1951, 2010

with 3–4 “holes” or sinkholes in the continental shelf that were discovered during a high-resolution SEABEAM survey in the austral summer of 2000–2001. The largest hole, hereafter referred to as the Commonwealth Bay Hole (CBH), is 875 m deep and isolated from the larger Adélie Depression below 375 m. It effectively traps the dense shelf water formed in this region in winter, as detected in during NBP00–08 (station 17) which found salinities as high as 34.77, greater than anything observed in the greater Adélie Depression during the wintertime occupation of 1999 or subsequent mooring deployments (Williams, 2004). This site has now been re-sampled by the French IPY-ALBION project with both ship-board CTD and moorings since 2007.

2.2 Water masses

The seasonal cycle of water mass transformations in the Adélie Depression is primarily driven by the annual growth and decay of sea ice (Williams et al., 2008a). In addition there is seasonally variable lateral input at mid-depths from warm modified Circumpolar Deep Water incursions across the shelf break and cold Ice Shelf Water from ocean/ice shelf interactions beneath the Mertz Glacier. Figure 3a–b shows the spatial distribution of mCDW and ISW from two high-quality ship-based summertime CTD surveys (NBP00–08 in January 2001 and A0803 in January 2008). The mCDW intensity, depicted as the potential temperature (°C) at the dissolved oxygen minimum within the mCDW layer ($28.00 < \gamma_n \times < 28.27\,\mathrm{kg\,m^{-3}}$), describes the transport of mCDW over the shelf break and into the AD through the eastern part of the Adélie Sill, and to a lesser extent into the Mertz Depression region (147–148.5° E). The mCDW signal weakens to the south and is not detected, using the before mentioned criterion, in stations against the coast, including the interior of Commonwealth Bay. Despite the evidence of a further intrusion to the east at 140° E, there is no evidence of this mCDW communicating across the Adélie Bank into the Adelie Depression. The spatial distribution of ISW, as indicated by potential temperatures colder than −1.94°C, extends northwestwards from Buchanan Bay, quickly losing its cold signature through mixing with the summertime water masses. As in the case of mCDW, we assume there is no direct influence of ISW

OSD
7, 1913–1951, 2010

into Commonwealth Bay, though both water masses are likely to be indirectly mixed into the local shelf water properties.

The seasonal change in vertical stratification is demonstrated in Fig. 3c with two summertime CTD profiles in Commonwealth Bay (station 17 and 62 from NBP00–08), and the CTD stations from over the Adélie Depression against the MGT that best represent the bulk winter properties (stations 27, 51, 84 from A9901). The locations of these stations are shown in Fig. 2b. The wintertime oceanography over the Adélie Depression is dominated by formation of dense shelf water at freezing temperatures and increasing salinity throughout the water column in response to polynya activity, with only minor contributions from mCDW and ISW (Williams and Bindoff, 2003; Williams et al., 2008a). The water column becomes near-homogenous in both salinity and temperature (see Fig. 3c–e). In summer the upper water column re-stratifies, as a warm, fresh and oxygen-rich Seasonal Mixed Layer (SML) forms at the surface from the wind driven convection of sea ice melt. The SML in Commonwealth Bay is the deepest for the region at ~350 m as reported by Vaillancourt et al. (2003). Station 17 in Commonwealth Bay also demonstrates the previously mentioned salinity maximum at depth within the Commonwealth Bay Hole. The main temporal gap in our observational datasets is the transitional period between these opposing seasons, in particular during autumn/fall when the heat content in the summer mixed layer must be eroded back to the freezing point for the onset of the new sea ice growth season. It is this specific time period that we will focus on in this paper.

OSD
7, 1913–1951, 2010

3 Datasets and Methods

3.1 Seal-derived CTD measurements

3.1.1 The SEaOS survey

The migration of the SEaOS and IMOS seals, equipped with autonomous CTD-Satellite Relay Data Loggers (CTD-SDRL) at Macquarie Island, to the AGV continental shelf is detailed in Fig. 2a. In late February 2005, two of nine SEaOS seals tracked from Macquarie Island entered the region near the Mertz Sill. In this paper we will refer to these SEaOS seals as S1 and S2, with corresponding GTS identification numbers 38 566 and 43 855, respectively. Seal S1 (green filled circles) surveyed the eastern sector of the Mertz Depression region and then exited the region between 146–147° E at the northern end of the series of grounded icebergs that extend from the MGT. Seal S2 (yellow circles) also entered the region through the Mertz Sill, but did not penetrate as far south into the Mertz Depression, remaining in the western sector of the sill region before moving to the western lee of the grounded icebergs near the Mertz Bank. Whereas seal S1 rapidly headed northwest away from the region, seal S2 migrated west just north of the shelf break along the upper continental slope. This trajectory is similar to those of icebergs transported by the Antarctic Slope Current (Aoki, 2003), which is often observed as a narrow, fast westward jet close to the 1000 m isobath (Williams et al., 2008a, 2010b).

3.1.2 The IMOS survey

In 2010, two of the fifteen IMOS seals equipped with CTD-SDRL instruments on Macquarie Island also chose to migrate south to the AGV region. In this paper we will refer to these SEaOS seals as I1 and I2, with corresponding GTS identification numbers 55 044 and 55 052, respectively. Both seals were originally heading SSE but between 12–14 February appear to change direction to SSW (see Fig. 1b). Interestingly this

OSD
7, 1913–1951, 2010

coincides with the reported timing of the calving of the MGT (B. Legrésy, personal communication, 2010). As in the case of the SEaOS seal, both IMOS seals approached the region through the Mertz Sill area, I1 (blue filled circles) entering through the centre and I2 (red filled circles) following two days later on the shallow topography to the west. Both seals then tracked closely, albeit 2–3 days apart, to the southern end of the grounded iceberg zone at 146° E and then along the northern flank of iceberg C–28 that had recently calved from the MGT en route to Commonwealth Bay at the end of February/ beginning of March. In Commonwealth Bay, I1 stayed in the eastern sector and departed (blue open circles) on the 26 March, collecting 55 profiles. I2 stayed nearly one month later, until the 26 April (thereafter red open circles), and occupied a wider area of Commonwealth Bay across both east and west sectors.

3.1.3 Instrumentation

As detailed in Boehme et al. (2008), the autonomous CTD-SDRLs used in the SEaOS and IMOS programs were constructed at the Sea Mammal Research Unit (SMRU) at the University of St Andrews, using a CTD sensor package built and calibrated by Valeport Ltd, Devon, UK. These units were harmlessly fixed to the seals fur after their annual moult in January/February. The data was relayed via the ARGOS system and distributed through the SMRU website. Previous studies have used comparisons of CTD-SDRL data with nearby ship-based CTD data to assess the accuracy of the salinity and temperature data. Unfortunately there is no useful ship-based data relevant to the timing and location of the data being used in this paper. Therefore following Boehme et al. (2008) we assume the uncertainty in both salinity and temperature to be 0.02. Basic post-processing was completed to remove all data points associated with density inversions in the profiles, with a 10% reduction in data. The assumption is made that the sensors are not accurate enough to detect instabilities in density due to the overturning from brine-rejection at the surface. One area of known problems is the location data associated with the CTD profiles and this will be addressed in future work involving state-spaced modelling. In this paper we use the original location data, which

OSD
7, 1913–1951, 2010

is clearly not prefect given the handful of point that are on land (see Fig. 2a: Inset), but sufficient for this particular study.

3.2 Estimation of heat content, flux and sea ice growth rates

Following Costa et al. (2008) we estimate the upper Ocean Heat Content (OHC, MJ m^{-2}) by calculating the heat content relative to the in situ freezing point (T–T_f) and integrating it to depth as follows:

$$\mathrm{OHC} = \rho c_p \int (T - T_f) dz \quad (1)$$

where ρ and c_p are the in situ density ($kg\,m^{-3}$) and specific heat of seawater ($J\,°C^{-1}kg^{-1}$). We then time difference this to get the OHC Flux ($W\,m^{-2}$).

We estimate sea ice production using the salinity budget method detailed in Charrassin et al. (2008).

$$\rho_o V_o S_o = \rho_o V_f S_f + \rho_i V_i S_i \quad (2)$$

where ρ_o is the sea water density = $1027\,kg\,m^{-3}$; V_o is the initial volume of water, with initial salinity S_o; V_i is the volume of ice formed with density ρ_i=$920\,kg\,m^{-3}$ and salinity 10; and $V_f = V_o - V_i$ is the final volume of the seawater with salinity S_f.

3.3 Environmental data

3.3.1 Satellite derived sea ice concentration

In this paper we use AMSR-E sea ice concentration data (AMSR-E, 2008) to examine the co-location of the seals movements to the open water areas of the Commonwealth Bay Polynya. Figure 4 shows the weekly mean sea ice concentration with corresponding seal locations from March through April. For the first few weeks there is relatively low sea ice concentration across the region. In week 1 the seals aggregate on both

OSD
7, 1913–1951, 2010

the western and eastern sectors. Towards the end of March the sea ice concentration is developing in the offshore region and the morphology of the Commonwealth Bay polynya takes definition in the central/eastern sector. This pattern is consistent in April and the seals are co-located with the region of greatest open water/lowest sea ice concentration.

3.3.2 AWS data from Cape Denison

For many years there has been an automatic weather station on the coast at Cape Denison (AWS, 2010) but the extreme wind regime has made it very difficult to collect robust and ongoing wind measurements[1]. For our study period there were no reliable wind measurements. In the Discussion section of this paper we present the available data for air temperature (°C) and air pressure (hPa). Ten-minute data was available across March through April, with a short break between 30 March and the 5 April.

4 Results

We present our results following the timing and trajectories of the seal data, specifically focusing on the new insights gained into the oceanographic processes of the region. Starting with the SEaOS deployment we show the shelf break seal-CTD transect in early March 2005, focusing on the temporal variability of the surface layer and zonal distribution of modified Circumpolar Deep Water exchange relative to near-repeat transects from ship-based surveys in the other seasons (see Fig. 2b). We then proceed to the more substantial IMOS results from 2010, where we examine two cross-shelf seal-CTD transects across the Adélie Depression and the subsequent repeat CTD

[1]"The Adélie coast is bad news," says Matthew Lazzara (principal investigator for the AWS program and Antarctic Meteorological Center at the University of Wisconsin-Madison). "Its a place to throw away hardware.", from The Antarctic Sun, http://antarcticsun.usap.gov/science/contenthandler.cfm?id=2031.

OSD
7, 1913–1951, 2010

profiling in Commonwealth Bay from March through April (see Fig. 2a). The initial IMOS seal-CTD profiles includes data collected zonally along the iceberg C–28 in the early stage after its calving from the MGT. The latter profiles describe the overturning of the seasonal mixed layer at the beginning of the new polynya/sea ice growth season, in particular estimating the upper ocean heat content and sea ice growth rates from basic heat and salinity budgets. The time-series of estimated daily sea ice growth rates are compared with the available meteorological and sea ice concentration data.

4.1 Seasonal distribution of Modified Circumpolar Deep Water Intrusions

Previous ship-based CTD surveys have provided some seasonal coverage of the shelf break region (see Fig. 2b). Figure 5 shows vertical sections of potential temperature for all four seasonal transects: A9901 (winter, panel A) with the RV *Aurora Australis* in August 1999, and NBP04–10 (spring, panel B) and NBP00–08 (summer, panels C) with the R/V *Nathaniel B Palmer* in October 2004 and January 2001, respectively. The CTD transect provided by the SEaOS seal movement complements these data by detailing the water masses and stratification in early March 2005 (panel E). An additional section is provided for NBP00–08 (summer) showing the dissolved oxygen (mL L^{-1}, panel D) to help delineate the warm/low oxygen mCDW signature at bottom-to-mid depths from the warm/high oxygen properties of the ice-free summer mixed layer at the surface. Though the transects are from different years and do not perfectly repeat in a region of abrupt changes in depth, they offer the most complete picture of the temporal and spatial variability in mCDW intrusions.

Starting in winter (Fig. 5a), the relatively small coverage between 143–146° E identified mCDW as warm as −1°C below 200 m that was strongest between 144–145° E, east of the Adélie Sill. In spring (panel B, late October 2004), the shelf-break transect showed weaker mCDW properties relative to August, related to the increase in shelf water from August–October through the last part of the sea ice growth season. The water column is predominantly cold, dense shelf water. For summer (panels C–D), the transect from NBP00–08 extended from 141–148° E and show the main core of warm,

OSD
7, 1913–1951, 2010

oxygen-poor mCDW over the Adélie Sill between 142–143° E. The SEaOS transect in early March covered a similar region and showed the warmest and most numerous mCDW signatures of all seasons. The same mCDW region east of the Adélie Sill was observed, however even stronger signals were detected upstream near the Mertz Sill (146–147° E), and downstream west of the Adélie Bank (140–141° E) near the entrance to the D'Urville Trough. The mCDW near the D'Urville Trough, and to a lesser extent at the Mertz Sill, is near 0 °C and indicative of the close proximity of the Antarctic Slope Front. This transect also shows the change in the vertical stratification of the Antarctic Surface Water (AASW) layer above the mCDW, in particular from 141–144° E (Fig. 5d). By March this warmer summer mixed layer has been eroded and the new cold winter mixed layer has started to form (Fig. 5e).

4.2 Upper water mass properties across the Adélie Depression in 2010 post-MGT calving

The MGT calved near 13th February 2010 after the mega-iceberg B9-b repositioned itself. The resulting 75 km iceberg C–28 had a short existence, breaking up further after the 10 March near the Adélie Sill before leaving the region completely. Both seals arrived in the Adélie Depression when C–28 had pivoted clockwise on its northern point, prior to its movement across the Adélie Depression, and completed ENE-WSW CTD-transects across the northern flank of C–28 en route to Commonwealth Bay. Vertical sections of salinity and potential temperature for these transects are shown in Fig. 6. In the Antarctic Surface Water (AASW) layer, from east (145–147° E) to west (143–145° E) there is a freshening of the layer and a deepening of the seasonal pycnocline that defines its base. This is likely to be the result of increased exposure to wind mixing and a greater amount of ice-free time closer to the coast in the west (Williams et al., 2008b, 2010b). The surface water is cooled to near the freezing point; the remnant summer mixed layer is observed in the west, at depths between 50–150 m between 144–145° E and in Commonwealth Bay between 142–143° E. Warm water anomalies below this depth are associated with mCDW intrusions which are more dominant in the

OSD
7, 1913–1951, 2010

north-east. There was no detection of Ice Shelf Water in potential temperature.

Both seals completed deep dives when near the C–28 iceberg, often diving to greater than 400 m. This is also the estimated depth of the iceberg. It is possible that the seals explored beneath the iceberg during these dives. While the profiles collected by seals in this location had the potential to observe ocean/ice shelf interaction, there was no detection of Ice Shelf Water (i.e. cold excursions from the surface freezing point in the vertical profiles of potential temperature). Seal I2 came the closest, as indicated in Fig. 6c–d. As introduced earlier, the volume of ISW is relatively small and the spatial impact on water mass properties are limited to the immediate region around Buchanan Bay. The seal CTD instruments would require greater precision to detect such subtle changes.

4.3 Initialisation of the winter mixed layer in Commonwealth Bay

The nine week occupation of Commonwealth Bay by seals I1 and I2 resulted in a unique dataset of CTD profiling through the upper ocean. In total, seals 44 and 52 collected 216 profiles of CTD within the Commonwealth Bay region from the 1 March to the 25 April (seal I1: 55 profiles from 1 March to 27 March and seal I2: 161 profiles from 2 March to the 25 April). The mean depth and standard deviation of these profiles were 324 ± 88 m and 367 ± 92 m for seals I1 and I2, respectively. Vertical sections of salinity, potential temperature ($^{\circ}$C) and potential density anomaly (kg m^{-3}), presented in Fig. 7, clearly show the erosion of the warm, fresh subsurface remnant of the summer mixed layer. The surface layer is already cold, indicating that the first phase of atmospheric cooling has already eroded the upper part of the summer mixed layer. Surface salinity increases from beginning of the record, indicating that the secondary phase of sea ice formation/brine-rejection has also already begun. There is a clear shoaling of the 34 isohaline through March until the week leading into April where there is a deepening and freshening/cooling.

OSD
7, 1913–1951, 2010

Figure 7 also presents the time evolution of the upper water column using vertical profiles of salinity (panel D) and potential temperature (°C, panel E) and combined $\theta - S$ space (panel F). The most dramatic changes occur in the surface layer, in conjunction with a broad shift in the deep water mass properties to colder, more saline values. The two historical casts from NBP00–08 (dark gray line) and A0803 (light grey line) are included. We note that seal I2 occupied the Commonwealth Bay hole in its deepest dive to >750 m, and recorded salinities higher than the NBP00–08 measurement. This qualitatively implies that there was more dense shelf water formation in 2009 than 2000. For potential temperature, it is clear that the surface layer was already cooled relative to the historical summertime profiles. In $\theta - S$ space, the data points collapse with time towards the freezing point line as the water column becomes relatively homogenous Shelf Water.

4.3.1 Upper ocean heat content and flux

The time-series in Fig. 7 show the conditioning of the remnant summer stratification in the preliminary development of the new winter mixed layer. We consider a 1-D model for the temperature budget and in Fig. 8 we present the Ocean Heat Content (OHC), i.e. how much heat is present in the upper water column at the summer/fall transition, and the Ocean Heat Content Flux (OHCF), i.e. the rate at which it changes. This is not to be confused with the ocean heat flux into the sea ice. In the absence of any lateral advection of heat into the region (via mCDW), the OHCF can be expected to decrease and asymptote as the water column is returned to the freezing point. Figure 8a shows the time-series of mean potential temperature across the upper 50 and 200 m, respectively, with the surface (6 m) values and corresponding in situ freezing point. The surface value reaches the freezing point on 13 March, though it is likely that sea ice growth has already started prior to this point, since the mean salinity is increasing at all levels from the 1 March (panel D). That this occurs when the temperature is not at the freezing point indicates that there is small-scale freezing occuring in the very surface/skin layer (0–6 m).

OSD
7, 1913–1951, 2010

The mean OHC (6–200 m) sampled over the Commonwealth Bay region is up to 400 MJ m^{-2} at the February/March transition and decreases to 50 MJ m^{-2} at the end of April. An 8-day running mean was applied to smooth the high frequency perturbations associated with the movement of the seal and internal dynamics within the survey area. We find a mean OHC flux of −100 W m^{-2} at the beginning of March, decreasing to 0 at the end of April. This implies that there is little of no advection of heat into the region from mCDW or otherwise at this time of the year. As in summer, Commonwealth Bay remains sufficiently removed from the major pathways of mCDW influence (see Fig. 3a).

4.3.2 Sea-ice growth rates

We estimate bulk daily sea ice growth rates over the area occupied by the seals in Commonwealth Bay during March and April using the simple 1-D salinity budget of Charrassin et al., 2008. This method assumes the effect of horizontal advection is negligible. Clearly full-depth profiles are required to capture the total change in salinity from brine-rejection. However we are limited to the dive depth of the seals and therefore this estimate will be conservative when the brine-driven overturning is deeper than our budget volume depth. In Fig. 8d–e we present the 8-day running mean time series of mean layer salinity (as in panel A) and inferred daily sea ice growth based on the 200 m and 300 m layers, which accounted for 98 and 76% of the available profiles, respectively.

The time series of mean layer salinity (panel D) shows how the increase in salinity at the surface convects, creating a new homogenous water mass from the top down. The surface and 50 m layer salinities are correlated through March, becoming more stratified between the 16–31 March and then less so thereafter. The 50 and 200 m layers converge approximately two weeks later. The record shows two major peaks in the inferred daily sea ice growth rates to greater than 10 cm day^{-1} around 8 March and 6–8 April, respectively.

OSD
7, 1913–1951, 2010

4.3.3 Correlating sea ice growth to meteorological and sea ice concentration data

From previous studies the meteorology of Commonwealth Bay is a combination of synoptic (warm low-pressure system from the north-west interacting with the cold, high-pressure system over Antarctica) and katabatic (cold, dense gravitational winds steered into this region by the upstream topography) processes. In terms of available data, we have at best the March through April record of air temperature and air pressure, with missing data between the 30 March and the 5 April (Fig. 9a). The trend upon both entering and leaving this data gap suggest that there was a low-pressure, increased air temperature event over this timeframe. The mostly negative correlation (Fig. 9b) between de-trended air temperature and pressure in the first period suggests the dominance of a synoptic regime, whereas in the second period (5–18 April) there is shift to a positive correlation, implying that there is now more input from the katabatic regime. That is, the pressure dropped significantly, but air temperatures remain cold, or decreased further, instead of increasing as expected from the synoptic regime.

We now consider the relationship between sea ice growth and sea ice concentration (Fig. 9c–d). The sea ice concentration is presented as the daily mean within a 10 km radius of the seal's location, and as the daily mean in the eastern sector of Commonwealth Bay. This region was identified earlier as being the centre of the low sea ice concentration in Fig. 4. The two estimates agree well, in particular during those times when the seals were sampling in the eastern sector. The correlation between concentration and growth is confused in March, but then has periods of significant ($p < 0.05$) negative correlation (29 March–4 April; 8–12 April and 17–20 April) in association with the increasing sea ice concentration. One explanation for this could be a potential negative feedback, whereby the polynya grows so much ice that the growth rate falls in relation to the ocean-atmosphere heat flux. The relationship between sea ice concentration and production is complex and requires greater analysis of the total surface energy budget, as in Renfrew et al. (2002).

OSD
7, 1913–1951, 2010

5 Discussion

5.1 Validation of satellite-derived sea ice growth rates

The assessment and monitoring of sea ice production in polynya regions is vital to our understanding of the polar climate, in particular the variability of the associated dense shelf water formations and its role in the meridional overturning circulation. Satellite-based studies of sea ice production offer the greatest coverage in time and space, but require in situ measurements from field-based studies for comparison. Sea ice production estimates were made by Williams and Bindoff (2003), for the polynya region adjacent to the MGT, using heat and freshwater budgets around a near-closed loop of ship-based CTD measurements. This result was based on an open water area of 20 km^2. Commonwealth Bay was not sampled during this experiment due to logistic constraints, as the sea ice was greater than 10 m thick. Therefore the sea ice growth estimates in this paper are unique, in both the timing (during the summer/fall transition) and location.

The most current satellite-based estimates of sea ice growth come the heat-flux algorithm for thin-ice presented by Tamura et al. (2007, 2008) using the NCEP-2 and ERA-40 datasets. Tamura et al. (2008) showed how these data agreed well the wintertime measurements from Williams and Bindoff (2003) over the region alongside the Mertz Glacier. Williams et al. (2010a) used these data to examine the regional variability of mean annual ice production from 1992–2005 and found that the Commonwealth Bay polynya had maximum annual production rates of ~15 m which produced on average 25–40 km^3 of sea ice per year, or 10–15% of the sea ice production over the Adélie Depression.

Here we compare the in situ estimates from this study with an update to the Tamura et al. (2008) estimates that now uses ERA-Interim data, instead of ERA-40 data, between 1992–2007 (Tamura et al., 2010). Figure 10 shows one standard deviation of the mean daily sea ice growth rates from 1992–2007 from NCEP-2 (dark gray shaded area) and ERA-Interim (light gray shaded area), respectively. The maximum daily

OSD
7, 1913–1951, 2010

growth rates for the same period are shown for each case as dark and light gray lines. For the purposes of this study we assume that these NCEP-2 and ERA-Interim estimates represent upper and lower bounds, respectively. The in situ measurements from this study include the 200 m and 300 m layer estimates from Fig. 9d, as blue and red lines, respectively. The satellite-derived mean daily sea ice growth rate is between 2–7 cm day^{-1}. While this is lower than the 10 cm day^{-1} peaks in the in situ estimates, the magnitude of the maximum daily growth rates are between 7–12 cm day^{-1} and are in good agreement.

This result is very promising for the long-term monitoring of satellite-derived sea ice growth. At the time of writing there was no estimates available for direct comparison in March–April 2010. When the data becomes available for the 2010 season there will be further opportunity to examine the temporal variability of the sea ice growth on shorter time-scales, in particular the 2–3 "peak events" discerned from the in situ estimates. Care will be needed in assessing the sources of error for both satellite-derived and in situ estimates. As discussed earlier our estimates are likely to be conservative because they are not based on the full-depth salinity budget. Additionally our method provides a bulk estimate over a wide area and is therefore likely to smooth over peak sea ice growth rates in the peak polynya regions against the coast. For example, helicopter-borne observations over the very core of the polynya region in Buchanan Bay alongside the Mertz Glacier in August 1999 estimated sea ice growth rates as high as 20 cm day^{-1} (Roberts et al., 2001).

5.2 New insights into the oceanography of the Adélie Depression

The seal-derived CTD data detailed in this study was unique in time and space and offers new insights into the oceanography of the region, in particular that of the Commonwealth Bay polynya. Typically the ship-based CTD data from Antarctic fieldwork is limited to the ice-free season in the austral summer. Surveys outside of this are rare and are relatively limited in their spatial coverage. For example the wintertime survey of the Adélie Depression in July–Sept. 1999 experienced very thick ice (>10 m) and

OSD
7, 1913–1951, 2010

was unable to reach the Commonwealth Bay at all. There have been advances in the ARGOS system with new Ice-ARGO floats capable of making CTD measurements beneath active sea ice outside of this period. However at this stage these are limited to depths greater than 2000–3000 m and therefore do not observe the coastal/continental shelf region. Similarly there are mooring arrays that offer year-round observations, such as the Mertz Polynya Experiment, but do not adequately observe the upper surface water column. In 2010 the IMOS seals sampled a unique region, at a unique time and did it continuously for nearly two months, providing the first observations of the water mass transformations beneath newly-formed sea ice during the summer/fall transition.

Williams et al. (2008a) referred to the late summer/early autumn period as the "conditioning" phase where the remnant summertime water masses are convected, first by atmospheric cooling and preliminary sea ice formation in preparation for the development of the winter mixed layer during the sea ice growth period in winter. However there was no direct measurement of this process since the shallowest instrument in this study was around 375 m. Whilst the technology for full-depth profiling mooring exists, they are not feasible in most polar regions due to the threat from icebergs. The IMOS seals have overcome this data gap, acting as virtual CTD profiler in the surface layer (consistently down to 300 m) in a polynya region against the Antarctic coast. Serendipitously there is an ongoing French mooring survey in Commonwealth Bay, due for retrieval in 2011, that in combination with these results will capture the salinity budget over the entire water column.

Ocean heat content has been estimated before from seal-mounted temperature sensors by Costa et al. (2008), specifically in the region of the West Antarctic Peninsula during the fall-winter period (April–August). Costa et al. (2008) showed there was strong variability over this region associated with the greater influence of Circumpolar Deep Water. Our study has shown that ocean heat content flux in Commonwealth Bay trends to zero after the remnant summer mixed layer has been eroded. This means the polynya is purely a latent-heat polynya. The implication that mCDW does not penetrate

OSD
7, 1913–1951, 2010

into this region agrees with the spatial distribution of mCDW from summertime surveys (Fig. 4). This is different to the polynya area over the greater Adélie Depression against the pre-calving position of the MGT, where Williams and Bindoff (2003) determined that mCDW, albeit highly modified through cross-shelf exchange with the newly formed winter mixed layer on the shelf, provided a small but detectable ocean heat flux to region.

The "work" done by a polynya during the summer-fall transition to re-condition the upper water column back to the near-surface freezing point is relative to the stratification of the water column, in particular the heat content, in conjunction with the air-sea flux. This in turn is related to two independent processes: the summer mixed layer and presence/absence of mCDW. Regions with shallow summer mixed layers and/or minimal penetration from mCDW can therefore be expected to start the sea ice growth season earlier. It follows that any regional changes to these processes in future climate scenarios will lead to the changes in the start of the sea ice growth season. More work is required to completely understand the temporal and spatial variability of mCDW around Antarctica relative to the major polynya regions.

5.3 Utilisation of oceanographic processes in elephant seal foraging behavior

This study has revealed not only physical oceanographic processes, but also shed some light onto how the Elephant seals are utilising these processes in their behavior. We would like to now suggest four physical processes that possibly influenced the foraging strategies, namely: the calving of the MGT; the Antarctic Slope Current; the cross-shelf pathways of modified Circumpolar Deep Water; and the late summer overturning of the upper surface layer in Commonwealth Bay. Beginning with the seal's response to the calving event, we showed in Fig. 1b that seals I1 and I2 both changed direction from SSE to SSW between the 11–14 February, which corresponds to the calving event of the MGT. The ocean is an excellent medium for the transmission of sound and there has been detection of calving events around Antarctica by acoustic instruments in West Australia (Gavrilov and Vazques, 2005) and beyond (Talandier

OSD
7, 1913–1951, 2010

et al., 2002). Of course only two out of fifteen of the IMOS seals decided to go to the AGV region. In addition, seals have visited the AGV region before in years when there wasn't a calving event, i.e. seals S1 and S2 from the SEaOS deployments. Nonetheless this was the first time that seals penetrated beyond the shelf break itself and both seals "investigated" the iceberg C–28 once there.

The second oceanographic process that is utilised by the seals, in particular in the SEaOS deployment, is the westward Antarctic Slope Current (ASC) over the upper continental slope. This region is documented around East Antarctica as having a narrow, fast-flowing westward jet (20–30 cm^{-1}) that is vertically homogenous and pinned to the 1000 m isobath (Williams et al., 2008b; Meijers et al., 2010; Williams et al., 2010b). Figure 2 showed that seal S2, after initially investigating the polynya region in the vicinity of the Mertz Bank and Mertz Depression, travelled westwards from 147–141° E. We estimate a mean speed of 17.5 $cm\,s^{-1}$ along this path, which is conservative given the extra time taken to complete 12 dives plus additional random movements. This is in reasonable agreement with the reported speeds of the ASC jet and suggests the seal was utilising this process in its movement.

In both SEaOS and IMOS deployments, the seals that travelled to the AGV region all approached the continental shelf break between 146–148° E. As discussed in an earlier section, this is a region of mCDW penetration across the shelf break. Based on these two surveys we speculate that this is the third oceanographic process the seals are using, i.e. the upwelling of warm, saline mCDW onto and across the continental shelf break, as a preferential pathway into the continental shelf region. Potential benefits include the energy saved by staying in warmer water and "going" with the flow. Again it is difficult to speculate on the robustness of this assertion with only two years of data. Future work is planned for examining the behavior of all the seals with respect to the shelf/slope interactions, in these and future deployments.

The repeat foraging in Commonwealth Bay in conjunction with the summer/fall reconditioning of the upper water column is final example of bio-physical coupling utilised by the IMOS seals. Given the short amount of time the SEaOS seals spent foraging

OSD
7, 1913–1951, 2010

in the early stage of the polynya near the Mertz Bank, we consider that something different was keeping the IMOS seals, in particular I2, diving and feeding in Commonwealth Bay for close to two months. One of the key summertime observations from the NBP00–08 survey in January 2001 was the deep chlorophyll maximum associated with well-developed seasonal (summer) mixed layer in the Commonwealth Bay region. This was attributed to the subduction from a shoreward driven Ekman transport that resulted from the strong south-easterly katabatic wind regime in this region (Vaillancourt et al., 2003; Sambrotto et al., 2003). One explanation for why the IMOS seals foraged so heavily in this region relates to this phenomenon. In our simple hypothesis (see Fig. 11) we suggest that in early summer the conditions in Commonwealth Bay promote elevated primary production that is ultimately pushed below the euphotic zone, possibly allowing even greater production to continue above. In the latter half of summer we suggest there could be increased secondary production in response to the primary production. Finally we conclude that when the water column begins to overturn during the summer/fall transition there is enhanced food availability for any seals, and possibly their prey, willing to stay within the growing pack of the new sea ice season.

6 Conclusions

Southern elephant seals (*Mirounga leonina*), fitted with Conductivity-Temperature-Depth sensors at Macquarie Island in January 2005 and 2010, collected unique oceanographic observations of the Adélie and George V Land continental shelf (140–148° E) from late February through April. In this paper we presented these data and the new insights gained into the oceanography of this region during the summer-fall transition. The seal data added a new late-summer snapshot from 2005 of the zonal distribution of modified CDW exchange across the shelf break, extending further east than previous observations, and showed a strong mCDW signal near 140° E in addition to previously documented. Seal transects across the Adélie Depression, including alongside iceberg C–28 that calved from the Mertz Glacier, demonstrated the late summer

OSD
7, 1913–1951, 2010

stratification with the SML in the surface and modified CDW at mid-depths. These highlighted the "work required" to return the water column to the winter state of full-depth homogeneity at the freezing point with increasing salinity from brine-rejection in the formation of dense shelf water. This was confirmed by the near-repeat CTD profiling conducted by the IMOS seals from March through April in Commonwealth Bay, one of the key polynya regions, which captured the convective overturning of the deep remnant SML at the beginning of the sea ice growth season. Heat and freshwater budgets were used to estimate the ocean heat content, heat flux and sea ice growth rates (7.5–12.5 cm s^{-1}). The heat content showed that the contribution of heat from advection was minimal and confirmed that Commonwealth Bay is primarily a latent-heat polynya region. We have demonstrated that these seal-derived data are invaluable in filling in previous gaps in our understanding of the temporal and spatial variability of the Antarctic coastal region. In particular the results in this paper will provide useful benchmarks for examining the satellite and model derived estimates of sea ice growth necessary for future monitoring and prediction of this important source region of Antarctic Bottom Water

Acknowledgements. This work was supported by the Marie de Paris "Research in Paris" program. SEaOS and IMOS Seal-CTD data was provided through Australian Animal Tracking and Monitoring System, a facility of Integrated Marine Observing System. The Australian Antarctic Division provided in-kind support. Field work was done in compliance with research permits supplied by the Tasmania Government's Department of Primary Industry, Water and the Environment. Animal ethics for all animal handling was approved by the University of Tasmania and Macquarie University's Animal Ethics Committees. Support for the NBP00–08 and NBP04–10 research voyages (contact S. S. Jacobs, Lamont-Doherty Earth Observatory, USA) was provided by the US National Science Foundation with the data processed and archived with the National Oceanographic Data Center. Support for the AU9901 (contact N. L. Bindoff, ACECRC, Australia) and AU0803 (contact S. R. Rintoul, CSIRO, Australia) research voyages provided by the Australian Antarctica Division. The authors would like to thank the officers, crew and technicians of the RVIB *Nathaniel B Palmer* and R/V *Aurora Australis* for their professional support in the collection of these observational data.

OSD
7, 1913–1951, 2010

The publication of this article is financed by CNRS-INSU.

References

Adolphs, S. and Wendler, G.: A pilot study on the interactions between katabatic winds and polynyas at the Adélie Coast, Eastern Antarctica, Antarct. Sci., 7, 307–314, 1995. 1917

AMSR-E: Daily Updated AMSR-E Sea Ice Maps, http://www.iup.uni-bremen.de:8084/amsr/amsre.html, 2008. 1922, 1944

Aoki, S.: Seasonal and Spatial Variations of Iceberg Drift off Dronning Maud Land, Antarctica, Detected by Satellite Scatterometers, J. Oceanogr., 59, 629–635, 2003. 1920

AWS: Cape Denison, http://amrc.ssec.wisc.edu/aws/capedenisonmain.html, 2010. 1923

Bailleul, F., Charrassin, J., Monestiez, P., Roquet, F., Biuw, M., and Ginot, C.: Successful foraging zones of southern elephant seals from the Kerguelen Islands in relation to oceanographic conditions, Philos. T. Roy. Soc. B., 1487, 2169–2181, 2007. 1915

Beaman, R.: A bathymetric Digital Elevation Model (DEM) of the George V and Terre Adélie continental shelf and margin, World Wide Web electronic publication, http://data.aad.gov.au/aadc/metadata/metadata_redirect.cfm?md=AMD/AU/GVdem_2008, 2009. 1942

Biuw, M., Boehme, L., Guinet, C., Hindell, M., Costa, D., Charrassin, J.-B., Roquet, F., Bailleul, F., Meredith, M., Thorpe, S., Tremblay, Y., McDonald, B., Park, Y.-H., Rintoul, S. R., Bindoff, N., Goebel, M., Crocker, D., Lovell, P., Nicholson, J., Monks, F., and Fedak, M. A.: Variations in behavior and condition of a Southern Ocean top predator in relation to in situ oceanographic conditions, Proceedings of the National Academy of Sciences of the United States of America, 104(34), 13705–13710, 2007. 1915

Boehme, L., Meredith, M. P., Thorpe, S. E., Biuw, M., and Fedak, M.: Antarctic Circumpolar Current frontal system in the South Atlantic: Monitoring using merged Argo and animal-borne sensor data, J. Geophys. Res., 113, C09012, doi:10.1029/2007JC004647, 2008. 1915, 1921

OSD

7, 1913–1951, 2010

Charrassin, J.-B., Hindell, M., Rintoul, S. R., Roquet, F., Sokolov, S., Biuw, M., Costa, D., Boehme, L., Lovell, P., Coleman, R., Timmermann, R., Meijers, A., Meredith, M., Park, Y.-H., Bailleul, F., Goebel, M., Tremblay, Y., Bostk, C.-A., McMahon, C. R., Field, I. C., Fedak, M. A., and Guinet, C.: Southern Ocean frontal structure and sea-ice formation rates revealed by elephant seals, Proceedings of the National Academy of Sciences of the United States of America, 105, 11634–11639, 2008. 1915, 1922, 1928

Costa, D. P., Klinck, J. M., Hoffman, E. E., Dinniman, M. S., and Burns, J. M.: Upper ocean variability in west Antarctic Peninsula continental shelf waters as measured using instrumented seals, Deep-Sea Res. Pt. II, 55, 323–337, 2008. 1915, 1922, 1932

ETOPO1: Global Predicted Bathymetry V11. Smith, W. H. F. and D. Sandwell, Global seafloor topography from satellite altimetry and ship depth soundings, Science, 277, 1956–1962, 1997., http://topex.ucsd.edu/marine_topo/, 2009. 1942

Gavrilov, A. and Vazques, G.: Detection and localization of ice rifting and calving events in Antarctica using remote hydroacoustic stations, in: Proceedings of ACOUSTICS 2005, 2005. 1933

Gordon, A. L. and Tchernia, P.: Waters of the continental margin off Adélie coast, Antarctica, Antarctic Research Series, Antarctic Oceanolgy II: The Australian-New Zealand Sector, edited by: Hayes, D. E., Washington, American Geophysical Union., J. Gascard and P. Chu, New York, Elsevier, 59–69, 1972. 1916

Kusahara, K., Hasumi, H., and Williams, G.: Impact of Mertz Glacier Tongue Calving on Dense Shelf Water, Nature Communications, submitted, 2010a. 1916

Kusahara, K., Hasumi, H., and Williams, G.: Dense Shelf Water Formation and Brine-Driven Circulation in the Adélie Depression, Ocean Modelling, 2010b. 1916

Marsland, S. J., Bindoff, N. L., Williams, G. D., and Budd, W. F.: Modeling water mass formation in the Mertz Glacier Polynya and Adélie Depression, East Antarctica, J. Geophys. Res., 109, C11003, doi:10.1029/2004JC002441, 2004. 1916

Marsland, S. J., Church, J., Bindoff, N. L., and Williams, G. D.: Antarctic coastal polynya response to climate change, J. Geophys. Res., 112, C07009, doi:10.1029/2005JC003291, 2007. 1916

Massom, R., Hill, K., Lytle, V. I., Worby, A. P., Paget, M. J., and Alison, I.: Effects of regional fast-ice and iceberg distributions on the behavior of the Mertz Glacier Polynya, East Antarctica, Ann. Glaciol., 33, 391–398, 2001. 1917

Mawson, D.: The Home of the Blizzard, Hodder and Stoughton, London,, "Abridged popular

OSD

7, 1913–1951, 2010

edition" of original published in 1915 by William Heineman, London; reprinted in facsimile in 1996 by Wakefield Press, South Australia, 438 pp., 1930. 1917
Meijers, A., Klocker, A., Bindoff, N. L., Williams, G. D., and Marsland, S. J.: The large-scale circulation off the East Antarctic coast (30–80 °E), "BROKE-West" a Biological/Oceanographic Survey Off the Coast of East Antarctica (30-80E) Carried Out in January-March 2006, Deep-Sea Res. Pt. II, 57, doi:10.1016/j.dsr2.2009.04.019, 2010. 1934
Meredith, M. P., Nicholls, K. W., Renfrew, I. A., Boehme, L., Biuw, M., and Fedak, M.: Seasonal evolution of the upper-ocean adjacent to the South Orkney Islands, Southern Ocean: results from a "lazy biological mooring", Deep-Sea Res. Pt. II, accepted, 2010. 1915
Parish, T. R. and Wendler, G.: The katabatic wind regime at Adélie Land, Int. J. Climate, 11, 97–107, 1991. 1917
Renfrew, I. A., King, J. C., and Markus, T.: Coastal polynyas in the southern Weddell Sea: Variability of the surface energy budget, J. Geophys. Res., 107(C6), 3063, doi:10.1029/2000JC000720, 2002. 1929
Rintoul, S. R.: On the origin and influence of Adélie Land Bottom Water. Ocean, Ice, and Atmosphere: Interactions at the Antarctic Continental Margin, Antarctic Research Series 75, edited by: Jacobs, S. and Weiss, R., Washington, American Geophysical Union, 75, 151–171, 1998. 1916
Roberts, A., Allison, I., and Lytle, V. I.: Sensible and latent heat flux estimates over the Mertz Glacier polynya, East Antarctica, from in-flight measurements, Ann. Glaciol., 33, 377–384, 2001. 1931
Sambrotto, R. N., Matsuda, A., Vaillancourt, R. D., Langdon, C., Brown, M., Measures, C., Jacobs, S. S., and Wells, H.: Summer plankton production and nutrient consumption patterns in the Mertz Glacier Region of East Antarctica, Recent investigations of the Mertz Polynya and George Vth Land continental margin, East Antarctica, Deep-Sea Res. Pt. II, 1393–1414, 2003. 1935
Talandier, J., Hyvernaud, O., Okal, E., and Piserchia, P.: Long-range detection of hydroacoustic signals from large icebergs in the Ross Sea, Antarctica, Earth Planet. Sc. Lett., 203, 519–534, 2002. 1933
Tamura, T., Ohshima, K. I., Markus, T., Cavalieri, D., Nihashi, S., and Hirasawa, N.: Estimation of thin ice thickness and detection of fast ice from SSM/I data in the Antarctic Ocean, J. Atmos. Ocean. Tech., 24, 1757–1772, 2007. 1930
Tamura, T., Ohshima, K. I., and Nihashi, S.: Mapping of sea ice production for Antarctic coastal

OSD
7, 1913–1951, 2010

polynyas, Geophys. Res. Lett., 35, L07606, doi:10.1029/2007GL032903, 2008. 1916, 1930, 1950

Tamura, T., Ohshima, K. I., Nihashi, S., and Hasumi, H.: Estimation of surface heat/salt fuxes associated with sea ice growth/melt in the Southern Ocean, Scientific Online Letter on the Atmosphere, submitted, 2010. 1930

Vaillancourt, R. D., Sambrotto, R. N., Green, S., and Matsuda, A.: Phytoplankton biomass and photosynthetic competency in the summertime Mertz Glacier Region of East Antarctica, Recent investigations of the Mertz Polynya and George Vth Land continental margin, East Antarctica, Deep-Sea Res. Pt. II, 1415–1440, 2003. 1919, 1935

Whitworth III, T.: Two modes of bottom water in the Australian-Antarctic Basin, Geophys. Res. Lett., 29, 1073, doi:10.1029/2001GL014282, 2002. 1916

Williams, G. D.: Adélie Land Bottom Water Production, Ph.D. thesis, University of Tasmania, 2004. 1918

Williams, G. D. and Bindoff, N. L.: Wintertime oceanography of the Adélie Depression, Recent investigations of the Mertz Polynya and George Vth Land continental margin, East Antarctica, Deep-Sea Res. Pt. II, 1373–1392, 2003. 1916, 1919, 1930, 1933

Williams, G. D., Bindoff, N. L., Marsland, S. J., and Rintoul, S. R.: Formation and export of dense shelf water from the Adélie Depression, East Antarctica, J. Geophys. Res., 113, C04039, doi:10.1029/2007JC004346, 2008a. 1916, 1918, 1919, 1920, 1932

Williams, G. D., Nicol, S., Raymond, B., and Meiners, K.: On the summertime mixed layer development in the marginal sea-ice zone off the Mawson coast, East Antarctica, Dynamics of Plankton, Krill, and Predators in Relation to Environmental Features of the Western Antarctic Peninsula and Related Areas, SO GLOBEC Part II., Deep Sea Res. Pt. II, 55(3–4), doi:10.1016/j.dsr2.2007.11.007, 365–376, 2008b. 1925, 1934

Williams, G. D., Aoki, S., Jacobs, S. S., Rintoul, S. R., Tamura, T., and Bindoff, N. L.: Antarctic Bottom Water from the Adélie and George V Land coast, East Antarctica (140–149° E), J. Geophys. Res., 115, C04027, doi:10.1029/2009JC005812, 2010a. 1916, 1930

Williams, G. D., Nicol, S., Aoki, S., Meijers, A. J. S., Bindoff, N. L., Iijima, Y., Marsland, S. J., and Klocker, A.: Surface oceanography of BROKE-West, along the Antarctic margin of the south-west Indian Ocean (30–80° E), "BROKE-West" a Biological/Oceanographic Survey Off the Coast of East Antarctica (30-80E) Carried Out in January-March 2006, Deep-Sea Res. Pt. II, 57, doi:10.1016/j.dsr2.2009.04.020, 2010b. 1920, 1925, 1934

OSD

7, 1913–1951, 2010

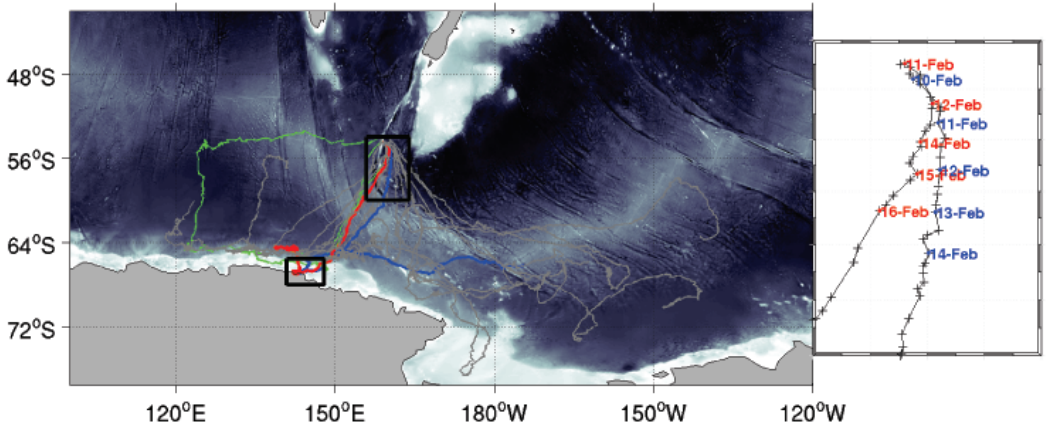

Fig. 1. Southern elephant seal tracks from IMOS in 2010 (grey lines). Specific seals that sampled the Adélie and George V Land continental shelf: seals I1 and I2 (blue and red lines, respectively), and SEaOS seals (2005) S1 and S2 (green lines). Inset: Change in direction of seals I1 and I2 (blue and red, respectively) after leaving Macquarie Island (start) in February 2010 from SSE to SSW in conjunction with the calving of the Mertz Glacier Tongue (MGT).

OSD
7, 1913–1951, 2010

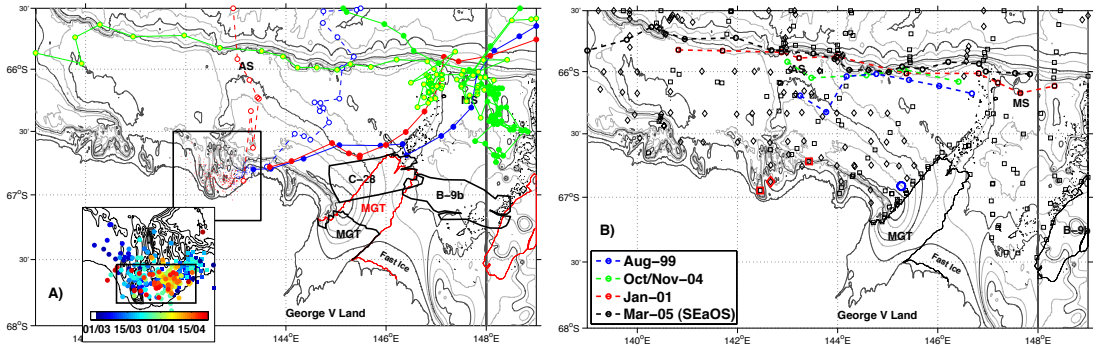

Fig. 2. Panel A: The Adélie Depression and surrounds with 500 m resolution bathymetry from Beaman (2009) between 139–148° E and ETOPO1 (2009) from 148–149° E. Major contour intervals shown for 4000, 3000, 2000, 1000, 500 and 200 m. The minor contour interval is 100 m and 200 m north and south of the 1000 m isobath respectively. Features include the Adélie Bank (AB), Adélie Depression (AD), the Adélie Sill (AS) and Mertz Sill (MS). Glacial features include the Mertz Glacier (MGT, pre-2010), iceberg B-9b and a fast ice region east of the MGT. Grounded icebergs indicated by black dots. The occupation of the Mertz Bank and Sill by SEaOS seals (S1 green-filled circles, S2 yellow-filled circles) and IMOS seals I1 and I2 (blue and red lines/circles, respectively) is shown. For the IMOS seals, filled circles/full lines indicate the pathway into the region (26–28 February) and the open circles/dashed lines indicate the exit pathway. The post-calving position of iceberg C28 on the 26 February is indicated by the thick black line (digitized from a MODIS image). Inset shows timing of seal CTD profiles in the Commonwealth Bay area, the black box indicating the limit of data used for sea ice growth estimates. Panel B: The location of high quality ship-borne summertime CTD measurements from NBP00–08 (squares) and AU0803 (diamonds). Specific CTD locations also shown for Fig. 3 from summer near Commonwealth Bay (NBP00–08, stations 17 and 61, red squares – AU0803, station 21, red diamond) and from winter near the MGT over the AD (AU9901, stations 27, 51 and 84, blue circles). Seasonal shelf break transects for Fig. 5 indicated by dashed lines for winter (AU9901, blue), spring (NBP04–10, green), summer (NBP00–08, red) and summer/fall (SEaOS, S2, black). The pre-calving position of the MGT and iceberg B9-b is shown in red. Pre-calving position of MGT and B-9b shown in black.

OSD
7, 1913–1951, 2010

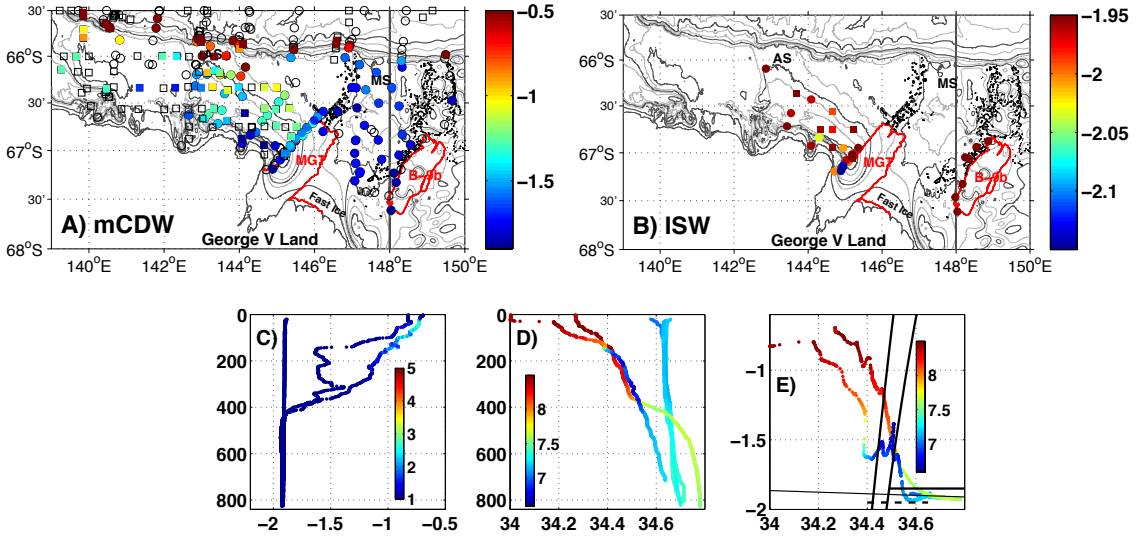

Fig. 3. Summary of regional water masses and seasonal stratification from historical ship-based CTD data. Planform distribution of mCDW (panel A) and ISW (panel B) from summertime CTD surveys (NBP00-08 and A0803). MCDW intensity indicated by potential temperature (°) at the dissolved oxygen minimum within the mCDW layer ($28.00 < \gamma_n < 28.27$). ISW intensity shown as potential temperature (< −1.94°C). Panels C–E shows characteristic vertical profiles and $\theta - S$ diagrams for summer (stations 17 and 61 from NBP00–08 in Commonwealth Bay) and winter (stations 27, 51 and 84 from A9901 over the Adélie Depression north of Watt Bay). Color scale is raw CTD-fluoresence for the vertical profile of potential temperature and dissolved oxygen (mL L^{-1}) for salinity and the $\theta - S$ diagram.

OSD
7, 1913–1951, 2010

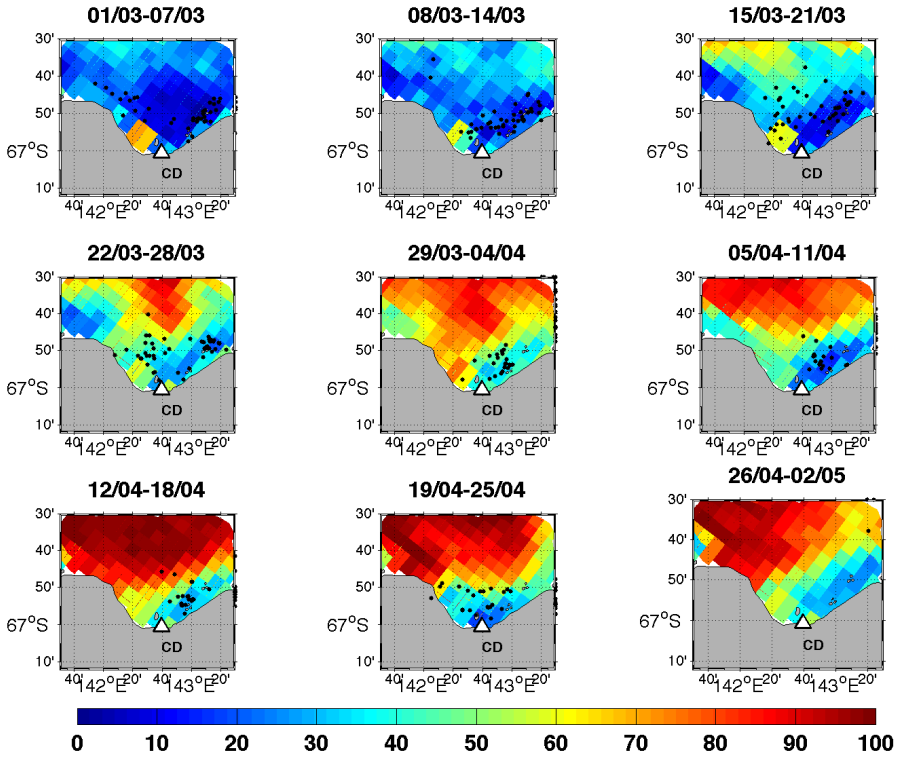

Fig. 4. Weekly locations of seals 44 and 52 (black dots) within Commonwealth Bay with mean sea ice concentration from AMSR-E (AMSR-E, 2008) from March through April 2010. Location of Cape Denison (CD) Automatic Weather Station as indicated by the triangle.

OSD
7, 1913–1951, 2010

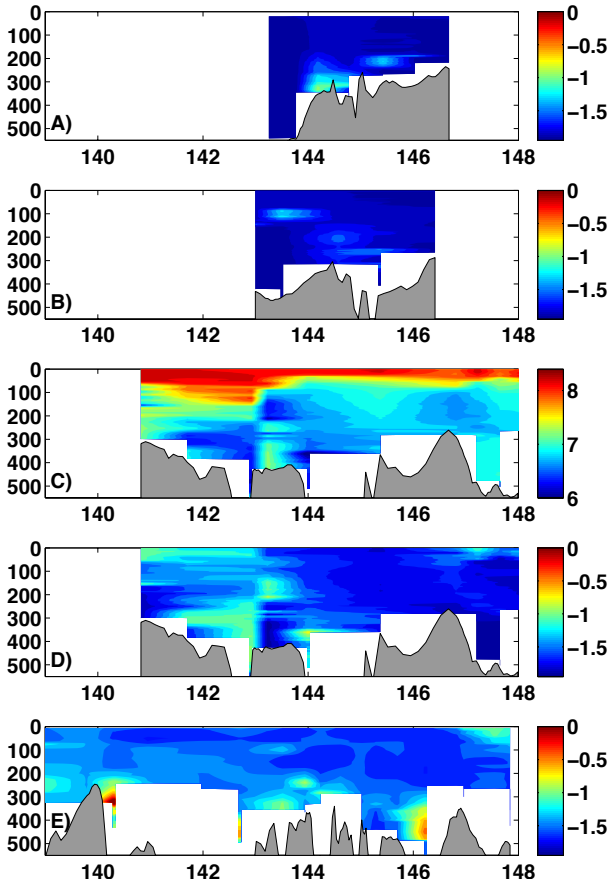

Fig. 5. Vertical sections of potential temperature (°C) across the AGV shelf break. Panels A–E (from top to bottom): winter (August 1999, A9901); spring (October 2004, NBP04–10); summer (January 2001, NBP00–08), dissolved oxygen (mL L^{-1}); summer, potential temperature; and summer/fall (March 2005, SEaOS).

OSD
7, 1913–1951, 2010

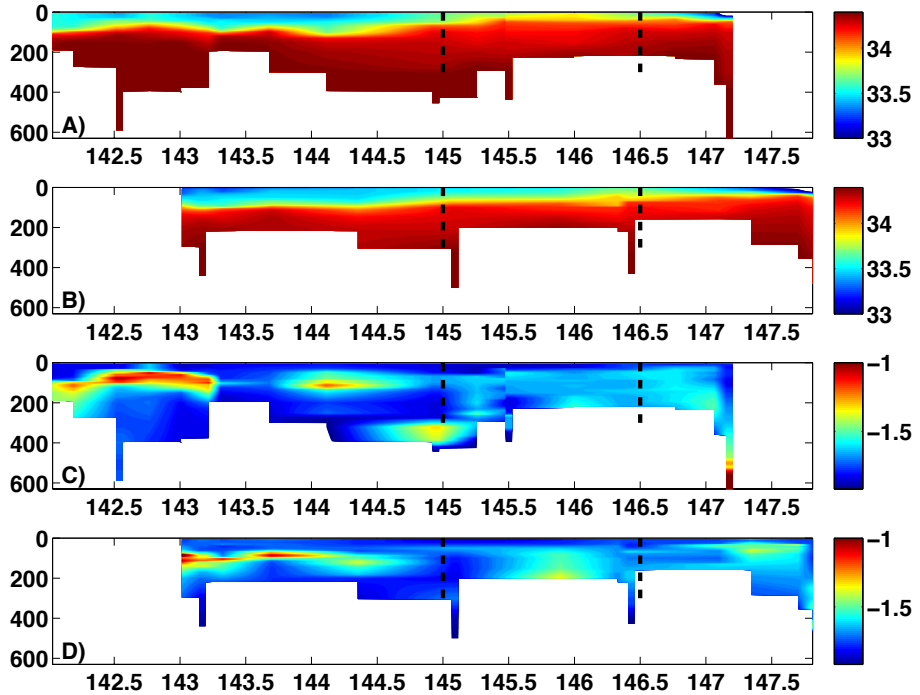

Fig. 6. Vertical sections of salinity (panels A–B) and potential temperature (C°, panels C–D) across the Adélie Depression 25–28 February from IMOS seals I1 and I2, respectively. Location of iceberg C–28 that calved from the MGT is between ~145–147° E.

OSD
7, 1913–1951, 2010

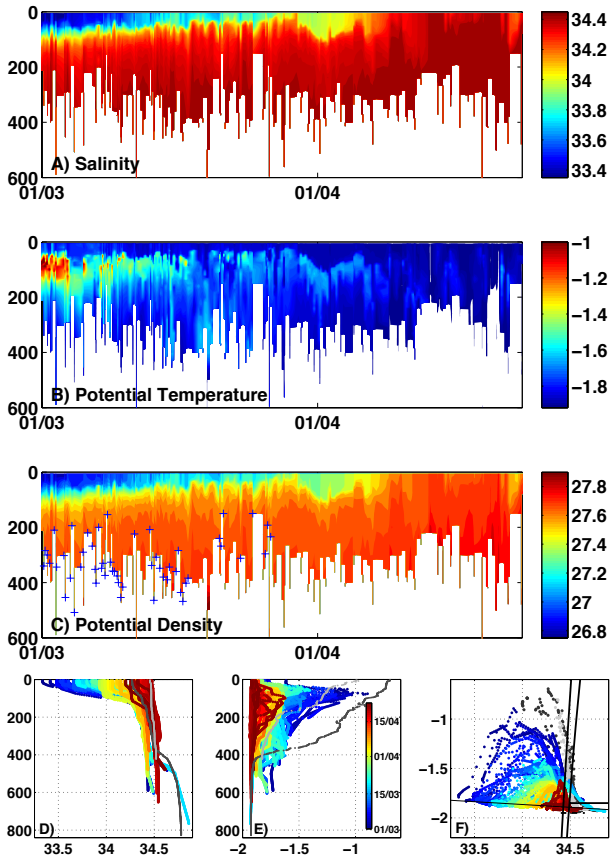

Fig. 7. Vertical sections of A. salinity, B. potential temperature (C°) and C. potential density (kg m^{-3}) for seal CTD data in Commonwealth Bay. Profiles collected by seal I1 indicated by blue '+' symbol. Lower panels: IMOS seal CTD data with nearest bottled calibrated ship based CTD data from NBP00–08 (station 17) and AU0803 (station 21), in dark and light gray, respectively. Panels D–E are vertical profiles of salinity and potential temperature (C°). Panel F is the $\theta - S$ diagram. Color scale on all panels is yearday of observation.

OSD
7, 1913–1951, 2010

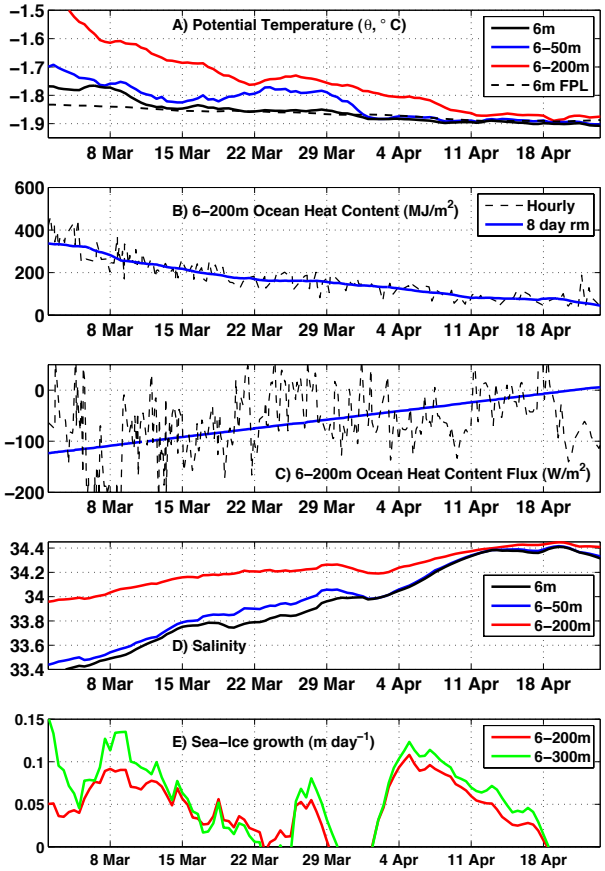

Fig. 8. Time series of (from top to bottom): **(a)** Potential temperature (°C, 4-day running mean) at the near-surface (6 m, black line) and averaged over the 6–50 m (blue) and 6–200 m (red) depth range. Near-surface freezing points shown as dashed black line; **(b)** Ocean heat content in the 6–200 m layer (MJ m^{-2}). Data shown is hourly (dashed black) and 8-day running mean (blue); **(c)** Ocean heat content flux (W m^{-2}); **(d)** as in **(a)**, but for salinity and E. Sea ice growth rates (m day^{-1}) from salinity budget. Estimates are for 6–200 m layer and 6–300 m layer (red and green, respectively).

OSD
7, 1913–1951, 2010

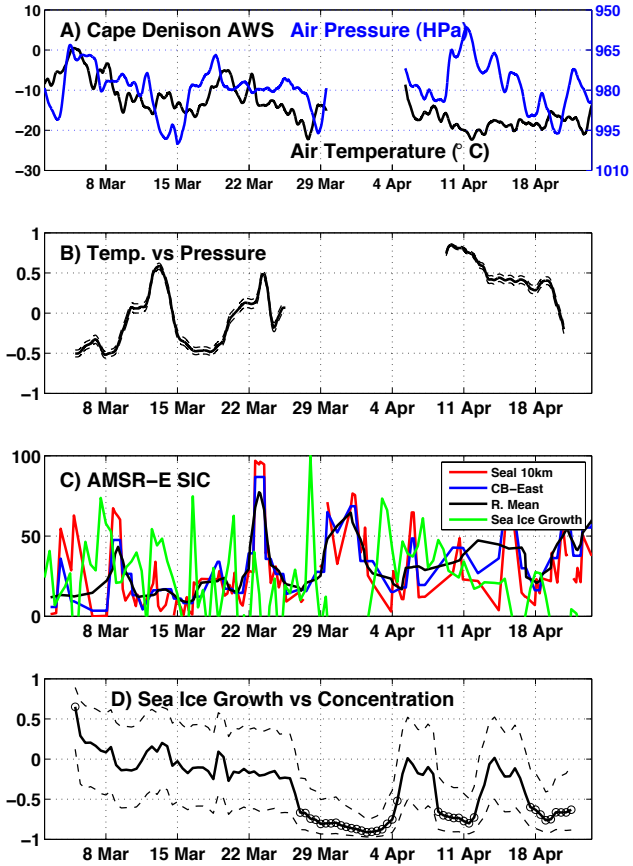

Fig. 9. Time series of: **(a)** AWS data from Cape Denison. Air pressure (HPa, blue) and air temperature (°C, black); **(b)** Correlation between air pressure and temperature. Dashed lines indicate 95% confidence level; **(c)** Sea ice concentration. Mean value within 10 km radius of seal locations (red) and eastern sector of Commonwealth Bay (blue, with 4-day running mean in black). Sea ice growth rates from Fig. 8 shown in green. **(d)** Correlation coefficients of sea ice growth with sea ice concentration. Dashed lines indicate 95% confidence level. Open circles indicate significant correlations ($p < 0.05$).

OSD
7, 1913–1951, 2010

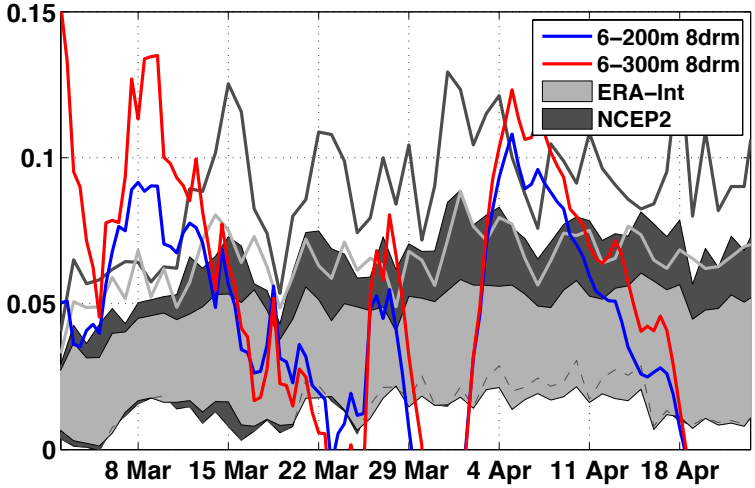

Fig. 10. Time series of estimated sea ice growth rates (m day^{-1}) from salinity budgets (6–200 m, blue and 6–300 m, red). Shaded areas are one standard deviation of the mean daily sea ice growth rates of Tamura et al. (2008) for 1992–2007 from NCEP–2 (dark gray shaded area) and ERA-Interim (light gray shaded area), respectively. Maximum daily values shown as thick lines (again, NCEP–2 is dark gray, ERA-Interim light gray).

OSD
7, 1913–1951, 2010

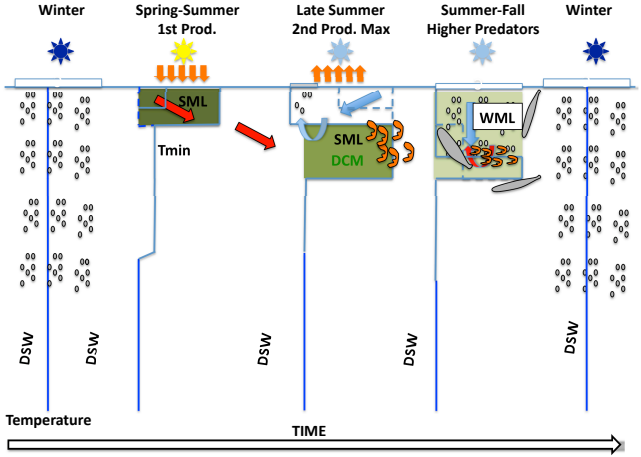

Fig. 11. Schematic of hypothesized processes that leads to the foraging behavior of the IMOS seals in Commonwealth Bay during the summer-fall transition (March through April). In winter the entire water column is near homogenous at the freezing point and gain salinity from brine-rejection. In summer a SML develops above the remnant winter mixed layer (or Tmin layer) and primary production is maximum at the surface. In Commonwealth Bay a particularly deep SML develops in conjunction with a Deep Chlorophyll Maximum (DCM). At the end of summer, atmospheric cooling brings the surface waters back to the freezing point, initiating sea ice growth and the development of the new winter mixed layer. During the summer-fall transition the remnant SML is eroded by convection of the upper layer. Our hypothesis is that the seals forage here at this time to take advantage of the secondary production (fish, krill etc) that have responded to the primary production of the DCM earlier in summer.

OSD
7, 1913–1951, 2010